

Observations and Predictions of HF Radio Propagation at High Latitudes

 $\begin{array}{c} \text{H.A.H. Al-Behadili} * ^{(1)(2)}, \text{E.M. Warrington} \overset{(2)}{\text{...}} \text{A.J. Stocker} \overset{(2)}{\text{...}}, \text{D.R. Siddle} \overset{(2)}{\text{...}}, \text{N. C. Rogers} \overset{(3)}{\text{...}}, \text{F. Honary} \overset{(3)}{\text{...}}, \text{N.Y. Zaalov} \overset{(4)}{\text{...}}, \\ \text{D.H. Boteler}^{(5)} \text{ and D.W. Danskin}^{(5)} \end{array}$

- (1) University of Misan, Amara, Iraq, http://www.uomisan.edu.iq/en/
- (2) University of Leicester, Leicester, UK, http://www.leicester.ac.uk
- (3) Lancaster University, Lancaster, UK, http://www.lancaster.ac.uk
- (4) St Petersburg State University, St Petersburg, Russia, http://www.spbu.ru
- (5) Geomagnetic Laboratory, Natural Resources Canada, Ottawa, Ontario, K1A 0Y3, Canada

Abstract

Space weather events can influence the ionospheric propagation of HF radiowaves in ways that are particularly pronounced at high latitudes. The most severe space weather events lead to a total loss of communications within the HF band (a radio blackout) via strongly enhanced D-region absorption. More commonly, events of intermediate severity can lead to disruption of communications that may be managed by appropriate frequency selection and by spatial diversity if the operational configuration is such as to allow this. At mid-latitudes, HF signals usually propagate on paths close to the great-circle between transmitter and receiver. However, at high latitudes the presence of various ionospheric features alters this behaviour. For example, the presence of patches of enhanced ionospheric electron density may reflect the signals into unexpected areas and can also shield particular regions from a given transmitter site. Our ray-tracing model as previously reported was based on goniometric measurements of azimuthal direction of arrival obtained in the 1990s. More recently, we have undertaken further measurements of signals received over a number of paths, including direction of arrival (both azimuth and elevation angles), time of flight (TOF) and signal strength with the specific aim of validating and developing our modelling procedures.

1 Introduction

Long range radio communications within the high-frequency (HF) band have been employed for many years for a range of applications, including point-to-point communications, radiolocation and over the horizon radar (OTHR). Such systems rely on the ionosphere as a propagation medium and the ability to estimate HF propagation behaviour is of critical importance when designing and operating radio systems in this band. Two aspects are of importance: ray path characteristics and radio wave absorption.

Space weather events can influence the ionosphere in a number of ways, and these can be particularly pronounced at high latitudes, i.e. within the auroral zone and polar cap [1]. The most severe space weather events lead to a total loss of communications within the HF band (a radio

blackout) via strongly enhanced D-region absorption. More commonly, events of intermediate severity can lead to disruption of communications that may be managed by appropriate frequency selection, relaying of messages, and by spatial diversity if the operational configuration allows this.

Our ray-tracing model as previously reported [2-4] was based on measurements of azimuthal direction of arrival obtained in the 1990s. More recently, we have undertaken further measurements of signals received over a number of paths (see Figure 1), including direction of arrival (both azimuth and elevation angles), time of flight (TOF) and signal strength with the specific aim of validating and developing our modelling procedures.

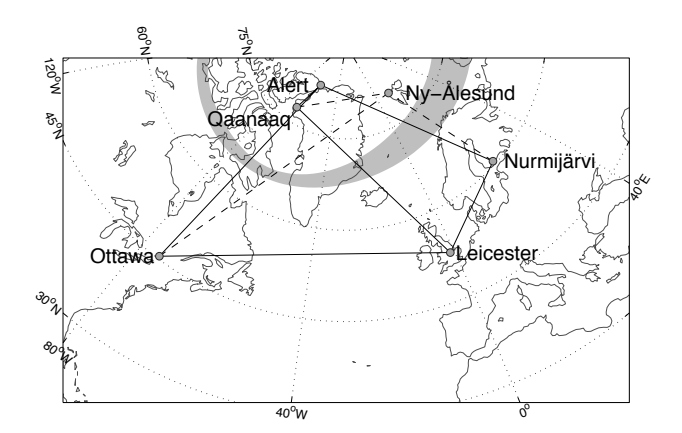


Figure 1. Map indicating our experimental configuration. Transmitters are located at Nurmijärvi, Qaanaaq and Ottawa, direction finding receivers at Alert and Leicester, and single channel receiver at Ny-Ålesund. The solid lines indicate the paths for which directional measurements are available, and the dashed lines those paths where only signal strength measurements are made.

The ionospheric ray-tracing model employed in this work has been described elsewhere [3], and the reader is directed to this source for a detailed description. Briefly, the main aspects of the model are summarised as follows:

• The simulations make use of a numerical ray tracing code [5] to estimate the ray paths through a model ionosphere. For the simulations presented here, the background ionosphere is produced by [6]

 The background model is then perturbed to include the various ionospheric features of interest, in particular patches and arcs of enhanced electron density, and, irregularities associated with the auroral oval and emedded in the wall of the trough.

HF absorption estimates are determined either from the NOAA D-Region Absorption Prediction (DRAP) model [7] that incorporates real-time X-ray and energetic proton flux measurements from the geostationary GOES-15 satellite, or the Polar Cap Absorption Model (PCAM) [8,9] which is a modification of DRAP that assimilates direct real-time absorption measurements from high-latitude riometers.

The area coverage to be expected from a transmitter at a given location is then estimated by ray-tracing through model ionospheres containing various features, including patches and arcs of enhanced ionisation and the sub-auroral trough. A large number of rays launched in an azimuth / elevation grid from the transmitter are traced through the model ionosphere. Each ray is assigned a power depending upon the transmitter power and antenna radiation pattern, absorption is added for each transit of the D-region taking into account the location and incidence angle of the transit, and the signal strength at the receiver estimated summing the ray power in the area around the receive antenna.

2 Measurements and Simulations

For the measurements reported in this paper, the transmitter was located at Qaanaaq and employed a nominal power of 100 W fed to an end-fed V broadband antenna. This type of antenna incorporates a resistive load as part of its design and is not as efficient as a resonant antenna. However, it was not possible for us to determine the precise efficiency of the antenna. Furthermore, the signal loss through various distribution systems at the receiver is unknown (and cannot be measured by the investigators due to the site location). Measurements of signal strength, direction of arrival and time of flight were made on a number of frequencies spanning the HF band.

An example period of measurements is presented in Figure 2 for a 7 MHz signal received over a path from Qaanaaq, Greenland to Alert, Canada (574km) for 6-14 January 2014. This period is one during which the absorption in the polar cap increased, but not such that a complete HF blackout occurred. The figure indicates various parameters observed during this period, namely (a) time of flight, (b) direction of arrival, (c) signal strength, (d) absorption predicted by the PCAM and DRAP models corrected for the oblique path, and (e) the lowest frequency (f_{min}) observed on the Qaanaaq ionograms (see [10]).

A clear variation in signal strength (Figure 2(c)) with a strong diurnal component is evident. At times away from the absorption event, there is good agreement with

VOACAP on the maximum signal strengths observed around local noon but the magnitude of the variation is underestimated. Furthermore, (as expected) VOACAP, being based on a statistical model, does not show any day-to-day variation over the period. Much reduced signal strength was observed for 8/9 January 2014, and less so on 10 January, corresponding to times of relatively high absorption but not so high as to completely absorb the signals.

An increase in the minimum observed frequency on the Qaanaaq ionosonde (Figure 2(e)) corresponding to the period of increased absorption is evident. This corresponds to an increase in the system dependent lowest usable frequency (LUF) for the ionosonde. [11] considered the effect of absorption on both vertical and oblique ionograms, and latterly [12] have considered employing vertical ionogram structure to optimize polar cap absorption models.

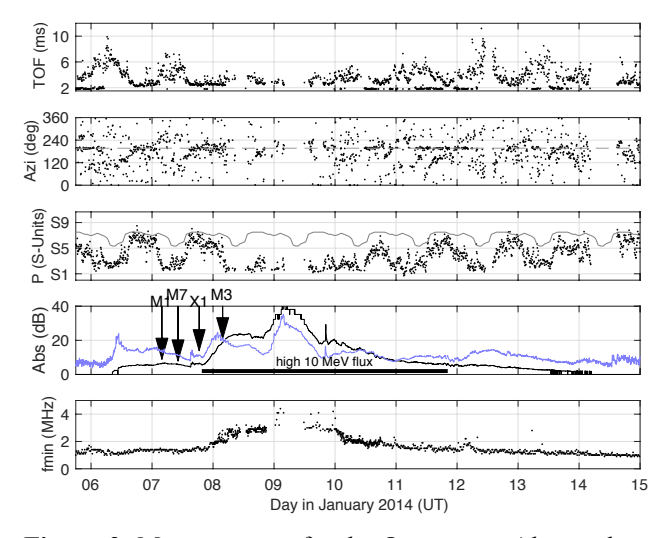


Figure 2. Measurements for the Qaanaaq to Alert path at 7.0 MHz for the period 6-15 January 2014 of (upper frame to lower frame): (a) signal time of flight, (b) the azimuthal angle of arrival, (c) signal strength (dots) and predicted signal strength using VOACAP (grey line), (d) absorption predicted by PCAM (blue line) and DRAP (black line) corrected for the oblique path, and (e) lowest observed frequency on the Qaanaaq ionosonde.

In Figure 2(d), the black curve represents the absorption of 7.0 MHz radiowaves predicted by the DRAP model corrected for slant propagation using the secant of the ray incidence angle. The DRAP model incorporates contemporary ('real-time') geomagnetic indices and satellite measurements of the solar X-ray and energetic proton fluxes. However, the ionospheric response parameters of the DRAP model (which can vary with D-region chemistry, electron temperature and layer structure) are constants based on climatological average values. The PCAM predictions (Figure 2(d), blue curve) optimised these parameters by assimilating real-time absorption measurements from the polar cap riometer at Taloyoak (69.5°N, 93.6°W geodetic), which measures

ionospheric absorption of 30 MHz cosmic noise and forms part of the Canadian Riometer Array [13].

The effect of the increased absorption of the coverage expected from the 7.0 MHz Qaanaaq transmitter at 1800 UT is illustrated in Figure 3 for 9 January 2014 (frame a) and 13 January 2014 (frame b), corresponding to a time of increased absorption and a time where the absorption has almost returned to normal levels.

The propagation mechanisms at 7.0 MHz during the period presented in Figure 2 are not straightforward. Periods of (mainly non-blanketing) sporadic E (Es) propagation are evident from the low times of flight (around 2 ms) displayed in frame (a) and the close to great circle propagation displayed in frame (b). Periods of ongreat circle F-region propagation are also evident, however periods when the propagation is well displaced from the great circle with associated large increase in the times of flight are also evident. It is interesting to note that there appears to be an underlying 24-hour period in the direction of arrival deviations and associated increases in the times of flight corresponding to excess path lengths of up to around 1500 km. There is no evidence of the much faster direction of arrival swings that are associated with convecting polar patches during this period.

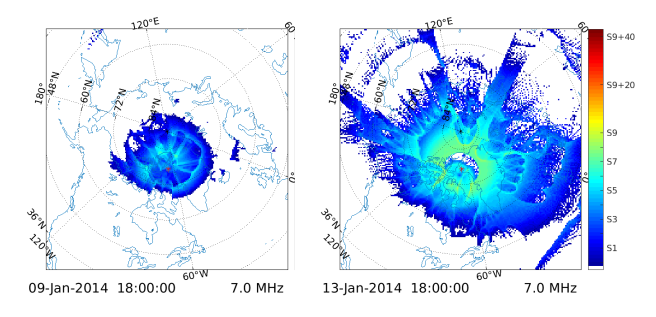


Figure 3. Coverage predicted for 7.0 MHz using the ray-tracing model for monopole antennas at both transmitter and receiver at (a) 18:00 UT, 9 January 2014, during the absorption peak, and (b) at 18:00 UT, 13 January 2014, absorption decayed to background levels.

The signal behaviour differs between the frequencies observed. At the lowest frequency, 4.6 MHz, deviations from the great circle path are much less than at 7.0 MHz, and there is very little evidence of long times of flight. The propagation characteristics at 8.0 MHz are very similar to those at 7.0 MHz. At 11.1 MHz, apart from Es, propagation is almost all off great circle with long times of flight. Above this frequency, at 14.4 MHz and 18.4 MHz, propagation is much reduced.

The 24-hour swings have only been observed on this shorter (574 km) path from Qaanaaq. This feature must be the result of a large-scale feature in the ionosphere, possibly due to reflections from a tongue of ionisation [14] extending from the dayside auroral zone to the pole. This feature is not currently in our models, but will need to be included in future versions.

Simulations for this 9-day period have been undertaken using the current version of our model outlined earlier. Periods of F-region propagation close to the GC direction are reasonably well predicted. Sporadic E (E_s) is not included in the model, and as such does not appear in the simulations and we have no independent measurements to determine its position and extent. Two-hop F-region modes are apparent in the predictions but not the measurements, as are short-period long delays at the beginning and end of normal propagation. The 2-hop features are some 20 dB weaker than the 1-hop, and as such are beyond the dynamic range of the Barker coded pulse scheme used in the measurements.

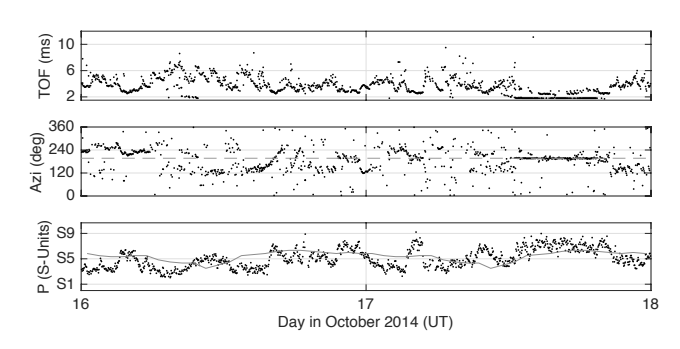


Figure 4. Measurements for the Qaanaaq to Alert path at 8.0 MHz for the period 16 and 17 October 2014 of (upper frame to lower frame): (a) signal time of flight, (b) the azimuthal angle of arrival, (c) signal strength (dots) and predicted signal strength using VOACAP (grey line).

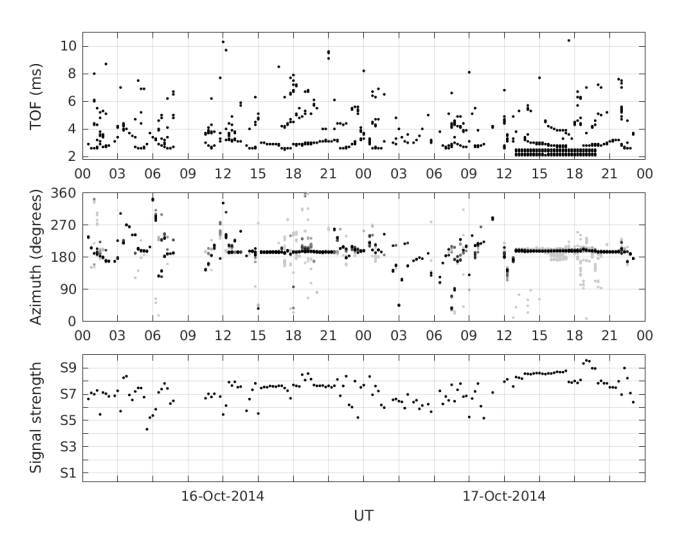


Figure 5. Time of flight, direction of arrival, and signal strength predicted for the Qaanaaq to Alert path by the ray-tracing model combined with DRAP absorption using one specific patch scenario for the period 16 and 17 October 2014 at 8.0 MHz.

Measurements for the 8.0 MHz signal are presented in Figure 4 for 16 and 17 October 2014. It is evident from this figure that the signal arrives at the receiver infrequently over the great circle path, often exhibiting swings in azimuth that are consistent with reflection from patches of enhanced ionisation convecting over the polar

region [15]. Associated with these swings are changes in the time of flight (TOF) of the signal, reaching a minimum value of around 2.5 ms when the azimuth passes through the great circle direction. The on-great circle traces with a TOF of around 2.0 ms, in particular after around 1200 UT on 17 October 2014, are associated with sporadic $E\left(E_s\right)$ propagation. The time of flight and the azimuth arrival angles derived from the model for the full 2 day period are shown in Figure 5. Whilst exact agreement is not expected (we don't know exactly where the patches are but do know the general area in which they are expected), the nature and magnitude of the azimuth and TOF variations agree reasonably well with the observed values.

3 Concluding Remarks

The overall aim of this work is to develop prediction techniques for nowcasting and forecasting purposes for HF radio systems operating in the high latitude (polar) regions that incorporate the mechanisms causing significant off-great circle propagation. The ray-tracing techniques adopted currently randomise the positions of the ionospheric features (patches, etc) as their exact number and positions are not known. The techniques can, however, be readily adapted to include positions based on measurements, such as may be obtained from the slant-TECs obtained from the IGS network.

The off-great circle propagation effects are important for two reasons: (a) they strongly influence the signal coverage, sometimes to the benefit of the system and sometimes not, and (b) several systems (e.g. DF and OTHR) rely on direction of arrival measurements usually (often erroneously) assuming it to be along the great circle path. Incorporating the off-great circle effects into the prediction code will assist in interpreting the measurements made by such systems.

4 Acknowledgements

The authors are grateful to the EPSRC for their support through grants EP/K008781/1 and EP/K007971/1. We are also grateful to the Global Ionospheric Radio Observatory [8] for the scaled ionosonde measurements, and to the Qaanaaq Geophysical Observatory for hosting the HF transmitter. A-CHAIM is supported under Defence Research and Development Canada contract number W7714-186507/001/SS and is maintained by the Canadian High Arctic Ionospheric Network (CHAIN) with operations support from the Canadian Space Agency. This research used the ALICE High Performance Computing Facility at the University of Leicester.

5 References

[1] R.D. Hunsucker, and J.K. Hargreaves, "The High-Latitude Ionosphere and its Effects on Radio Propagation", Cambridge University Press, 2003.

- [2] N.Y. Zaalov, E.M. Warrington and A.J. Stocker, "Simulation of off-great circle HF propagation effects due to the presence of patches and arcs of enhanced electron density within the polar cap ionosphere", *Radio Science*, **38**, 3, 1052, 2003.
- [3] N.Y. Zaalov, E.M. Warrington and A.J. Stocker, "A ray-tracing model to account for off-great circle HF propagation over northerly paths", *Radio Science*, **40**, 4, RS4006, 2005.
- [4] H.A.H. Al-Behadili, "Propagation Model for Nowcasting of HF Communications with Aircraft on Polar Routes", PhD thesis, Department of Engineering, University of Leicester, 2018.
- [5] R.M. Jones and J.J. Stephenson, "A Versatile Three-Dimensional Ray Tracing Computer Program for Radio Waves in the Ionosphere", Office of Telecommunications, OT 75-76, U.S Department of Commerce, Washington, USA, 1975.
- [6] D.R. Themens, P.T. Jayachandran, A. McCaffrey, and B. Reid, "The Assimilation Canadian High Arctic Ionospheric Model (A-CHAIM) (U)," DRDC-RDDC-2020-C045, 2020.
- [7] H.H. Sauer and D.C. Wilkinson, "Global mapping of ionospheric HF/VHF radio wave absorption due to solar energetic protons", *Space Weather*, **6**, S12002, 2008.
- [8] N.C. Rogers and F. Honary, "Assimilation of realtime riometer measurements into models of 30 MHz polar cap absorption", *Space Weather and Space Climate*, **5**, A8,2015.
- [9] N.C. Rogers, A. Kero, F. Honary, P.T. Verronen, and E.M. Warrington, "Improving the twilight model for polar cap absorption nowcasts", *Space Weather*, 14, pp 950-972, 2016.
- [10] B.W. Reinisch and I.A. Galkin, "Global ionospheric radio observatory (GIRO)", *Earth Planets Space*, **63**, 4, pp 377-381, 2011.
- [11] N.Y. Zaalov, E.V. Moskaleva, D.D. Rogov and N.N. Zernov, "Influence of X-ray and polar cap absorptions on vertical and oblique sounding ionograms on different latitudes", *Advance in Space Research*, **56**, 11, pp 2527-2541, 2015.
- [12] N.Y. Zaalov and E.V. Moskaleva, "A polar cap absorption model optimization based on the vertical ionograms analysis", *Advance in Space Research*, **58**, 9, pp 1763–1777, 2016.
- [13] D.W. Danskin, D. Boteler, E. Donovan, and E. Spanswick, "The Canadian riometer array". Proc. 12th International Ionospheric Effects Symposium (IES 2008), Alexandria, VA, USA, pp 80–86, 2008.
- [14] H.R. Middleton, S.E. Pryse, L. Kersley, G.S. Bust, E.J. Fremouw, J.A. Secan, and W.F. Denig, "Evidence for the tongue of ionization under northward interplanetary magnetic field conditions", *Journal of Geophysical Research*, 110, A07301, 2005.
- [15] E.M Warrington, N.C. Rogers and T.B. Jones, "Large HF bearing errors for propagation paths contained within the polar cap," *IEE Microwave Antenna P*, **144**, 4, pp 241-249, 1997.